Am J Physiol Regul Integr Comp Physiol 305: R793–R803, 2013.
First published May 29, 2013; doi:10.1152/ajpregu.00549.2012.

Orientation within a high magnetic field determines swimming direction and laterality of c-Fos induction in mice

Thomas A. Houpt,[1] Bumsup Kwon,[1] Charles E. Houpt,[1] Bryan Neth,[2] and James C. Smith[2]

[1]*Department of Biological Science, Program in Neuroscience, The Florida State University, Tallahassee, Florida; and* [2]*Department of Psychology, Program in Neuroscience, The Florida State University, Tallahassee, Florida*

Submitted 29 November 2012; accepted in final form 24 May 2013

Houpt TA, Kwon B, Houpt CE, Neth B, Smith JC. Orientation within a high magnetic field determines swimming direction and laterality of c-Fos induction in mice. *Am J Physiol Regul Integr Comp Physiol* 305: R793–R803, 2013. First published May 29, 2013; doi:10.1152/ajpregu.00549.2012.—High-strength static magnetic fields (>7 tesla) perturb the vestibular system causing dizziness, nystagmus, and nausea in humans; and head motion, locomotor circling, conditioned taste aversion, and c-Fos induction in brain stem vestibular nuclei in rodents. To determine the role of head orientation, mice were exposed for 15 min within a 14.1-tesla magnet at six different angles (mice oriented parallel to the field with the head toward B+ at 0°; or pitched rostrally down at 45°, 90°, 90° sideways, 135°, and 180°), followed by a 2-min swimming test. Additional mice were exposed at 0°, 90°, and 180° and processed for c-Fos immunohistochemistry. Magnetic field exposure induced circular swimming that was maximal at 0° and 180° but attenuated at 45° and 135°. Mice exposed at 0° and 45° swam counterclockwise, whereas mice exposed at 135° and 180° swam clockwise. Mice exposed at 90° (with their rostral-caudal axis perpendicular to the magnetic field) did not swim differently than controls. In parallel, exposure at 0° and 180° induced c-Fos in vestibular nuclei with left-right asymmetries that were reversed at 0° vs. 180°. No significant c-Fos was induced after 90° exposure. Thus, the optimal orientation for magnetic field effects is the rostral-caudal axis parallel to the field, such that the horizontal canal and utricle are also parallel to the field. These results have mechanistic implications for modeling magnetic field interactions with the vestibular apparatus of the inner ear (e.g., the model of Roberts et al. of an induced Lorenz force causing horizontal canal cupula deflection).

magnetic field; vestibular; brain stem; swimming; c-Fos

HIGH-STRENGTH MAGNETIC FIELDS typical of magnetic resonance imaging (MRI) machines can perturb the vestibular system of humans and rodents. Workers and subjects report vertigo, dizziness, or nausea around and within MRI machines of 4 tesla (T) and above (4, 5, 8, 10, 18, 26, 29, 30). At higher field strengths, subjects report sensations of falling or rotation, especially during movement through steep, magnetic field gradients (10, 22). Deficits in visual-motor tasks performed around MRI machines have also been reported that may be related to vestibular effects of the magnetic field (6, 7, 9).

Recordings of nystagmus have provided objective evidence of vestibular responses to magnetic field exposure in humans. During a blood oxygenation-level-dependent (BOLD) study of responses to caloric stimulation of the inner ear, spontaneous nystagmus was observed within a 1.5-T MRI machine, and subjects also reported "illusory perception of tilt" after magnetic field exposure (21). When exposed to 3 T or 7 T in the dark (i.e., in the absence of visual fixation), subjects showed horizontal nystagmus that was dependent on the orientation of the head within the MRI machine (24). The nystagmus was transiently reversed when the subjects were removed from the MRI machine. Subjects with bilateral loss of labyrinth function did not show nystagmus in the MRI machine, supporting a direct interaction of the magnetic field with the peripheral vestibular apparatus.

In rodents, we have found that exposure to static magnetic fields of 7 T or greater induced circular locomotion (15, 16), conditioned taste aversion (CTA) (16), and c-Fos induction in the vestibular nuclei of the brain stem (28). These effects are consistent with vestibular perturbation induced by more conventional stimuli such as whole-body rotation. Furthermore, chemical labryinthectomy abolishes responsiveness of rats to the magnetic field, again supporting a direct role for the inner ear (2, 14).

Previous studies have also found a critical role for orientation relative to the magnetic field. After magnetic field exposure with the rostral-caudal body axis parallel to the magnetic field and with the head toward B+, rats and mice walk or swim in counterclockwise circles (15, 16). Conversely, when exposed with the head toward B− (achieved either by inverting the animal within a superconducting magnet or inverting the polarity of the magnetic field within a resistive magnet), rats walk in clockwise circles (16). Rats also tilt their heads during magnet exposure, with the head tilted to the right when exposed head-up toward B+, but tilted to the left when exposed head-down toward B− (13). Furthermore, rats do not walk in circles nor do they acquire CTA after being exposed with the rostral-caudal axis perpendicular to the magnetic field (i.e., sideways, with dorsal side up within a large, resistive magnet) (17). These results from rodents suggest a critical dependence on orientation for vestibular stimulation and for the aversive effects of magnetic field exposure.

These results are consistent with the recent demonstration that horizontal nystagmus in humans within a 7-T MRI machine varies with the subject's orientation (24). The direction of nystagmus depends on orientation relative to the static magnetic field, and is reversed when the orientation of the subject is reversed (i.e., head toward B+ vs. B−). The slow-phase velocity of nystagmus is maximal when the head is pitched anteriorly up (backward) 20° in a supine subject, but nystagmus is absent when the head is pitched anteriorly down (forward) by 30°. Thus as in rodents, vestibular perturbation by high magnetic fields in humans is modulated by orientation and

Address for reprint requests and other correspondence: T. A. Houpt, Dept. of Biological Science, King Life Sciences Bldg., 319 Stadium Dr., The Florida State Univ., Tallahassee, FL 32306-4295 (e-mail: houpt@neuro.fsu.edu).

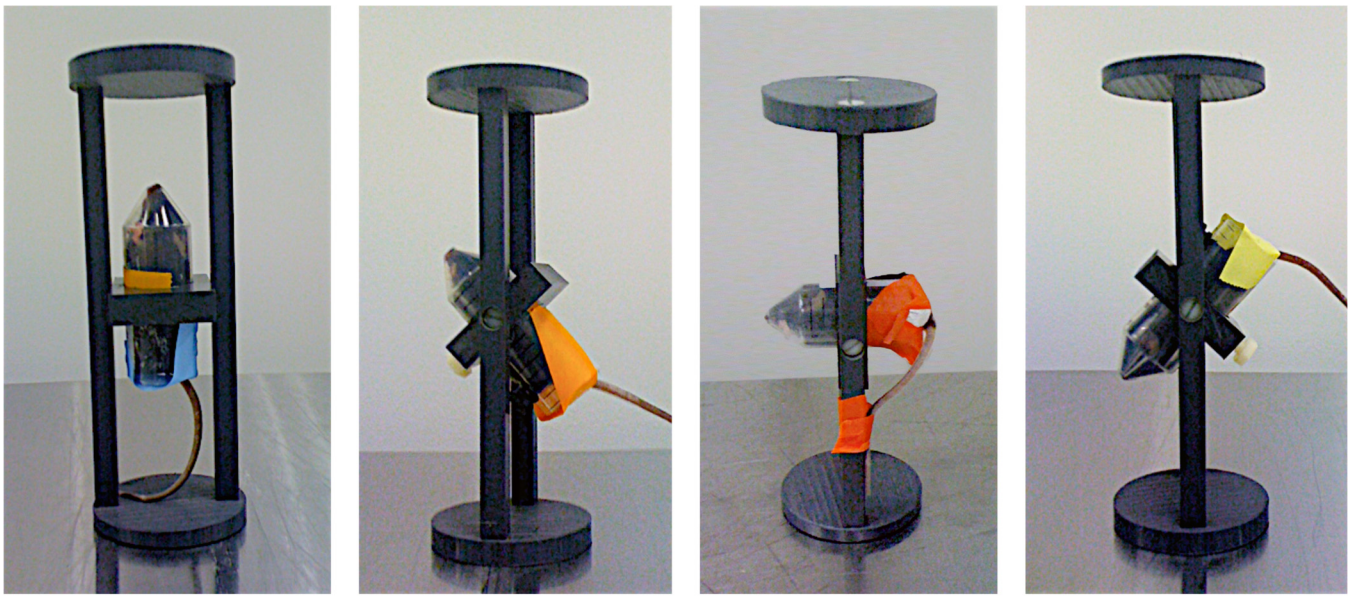

Fig. 1. Examples of mice restrained in a 50-ml conical tube secured in a plastic holder at different angles. At 0°, mice were positioned head up with the rostral-caudal axis parallel to the magnetic field. At 90°, mice were positioned sideways with the rostral-caudal axis perpendicular to the magnetic field lines. Mice could also be positioned at intermediate angles (e.g., at 45° and 135°).

specifically by the relative position of the head with respect to the magnetic field.

To further define the dependence of vestibular effects on orientation, we exposed mice to a 14.1-T magnetic field while they were restrained at different angles (0°, 45°, 90°, 135°, and 180°) relative to the magnetic field lines. We measured circling immediately after exposure during a 2-min swimming test, which maximizes limb movements and locomotion while minimizing spatial and gravitational cues (15). We also measured c-Fos induction in vestibular and visceral nuclei of the brain stem to determine whether neural activation paralleled the behavioral response after exposure at three different angles (0°, 90°, and 180°).

METHODS

Animals

Adult male C57BL/J mice (20–25 g; Jackson Laboratories, Bar Harbor, ME) were housed individually in polycarbonate cages in a temperature-controlled (22 ± 2°C, 30–40% humidity) colony room at the US National High Magnetic Field Laboratory at Florida State University. The mice were maintained on a 12-h light/dark cycle with lights-on at 7:00 A.M. All procedures were conducted during the light cycle. The mice had ad libitum access to Purina Rodent Chow and deionized-distilled water. All procedures were approved by the Florida State University animal care and use committee.

Magnet

Exposure to the high magnetic field was conducted with a superconducting magnet with a vertical bore designed for biochemical nuclear magnetic resonance studies. The 14.1-T magnet was a 600 MHz Bruker Cryo magnet with an 89-mm bore and fixed field strength of 14.1 T. It contained a shim magnet extending along the magnet bore for approximately 15 cm from the magnet's core, which was used to stabilize the magnetic field and give the central core field uniform strength. The magnetic field was oriented vertically so that the positive pole (B+) was at the top of the magnet. The magnet was operated without radiofrequency pulses, so mice were exposed only to static magnetic fields.

Before exposure to the magnetic field (magnet exposure) or sham exposure, mice were restrained by being placed in a plastic tube made from a 50-ml conical centrifuge tube, with the head of the mouse positioned at the cone end (20). The end of the conical tube subtends a 60° angle, so that the head of the restrained mouse was pitched downward rostrally by 30°. A hole in the tip of the cone allowed for breathing. A plastic plug with a hole to allow for the tail of the mouse at the caudal end of the tube restrained the mouse from moving. The restraint tube was held in a plastic frame that allowed the tube to be oriented at arbitrary angles, from 0° (straight up) to 180° (straight down; see Fig. 1 for examples.) During exposure in the magnet, mice were exposed to ambient light entering the top of the magnet's bore from the ceiling lamps of the room, although exposure was restricted by the relatively small diameter of the bore and the opaque plastic frame holding the restraint tube.

Experiment 1: Swimming After Magnetic Field Exposure

Mice (n = 30) were individually placed in the restraint tube and placed in the center of the 14.1-T magnet at one of five angles (0°, 45°, 90°, 135°, 180°; n = 6 at each angle) relative to the magnetic field lines, where 0° was parallel to the field lines pointing toward the top of the magnet (B+). The relative orientation of the body axes for each position is shown in Table 1.

Table 1. *Orientation of head and body axes of mice relative to magnetic field at different angles of restraint*

Restraint Angle	Head Direction	Rostral-Caudal*	Dorsal-Ventral*	Interaural*
0°	B+	∥	⊥	⊥
45°	B+	45°	45°	⊥
90°	Neutral	⊥	∥	⊥
90° sideways	Neutral	⊥	⊥	∥
135°	B−	135°	45°	⊥
180°	B−	∥	⊥	⊥

The head of the mouse was pitched rostrally down 30° from the horizontal (rostral-caudal) plane within the cone of the restraint tube. *Body axis relative to magnetic field lines; ⊥, perpendicular; ∥, parallel.

An additional group of mice (90° sideways, $n = 5$) were placed in the magnet angled sideways with their right side toward B+ (i.e., with the rostral-caudal and dorsal-ventral axes perpendicular to the magnetic field, but with the interaural axis parallel to the field lines).

Mice were inserted into the bottom of the vertical bore of the magnet, then quickly raised through the magnet until they were in the core of the magnet. Mice remained in the 14.1-T magnetic field for 15 min. As sham controls, mice were restrained and placed for 15 min in a head-up ($n = 3$) or head-down ($n = 3$) position in an opaque polyvinyl chloride tube in the animal colony (i.e., in the absence of the high magnetic field, although still exposed to the ambient geomagnetic field of ~48 μT).

After magnet or sham exposure, each restrained mouse was carried 50 m from the magnet to the animal facility in ~30 s, removed from the restraint tube, placed in the center of a circular swimming pool (1 m diameter; 30 cm depth) filled with water at room temperature, and allowed to swim for 2 min.

Mice were videotaped from above with a digital camcorder (Sony DCR-HC53) mounted above the swimming pool. After the swim test mice were returned to their home cage, which was positioned under a heat lamp, until they were dry. All mice were tested only once.

For quantitative analysis, the videotapes of mice swimming were later digitized onto a Macintosh computer using the QuickTime Player program (Apple) at a rate of 30 frames per s. Each frame of the digitized video was 640 pixels wide by 480 pixels tall, giving a spatial resolution of 4 pixels/cm. A custom software program (15) was used to automatically determine the position of the mouse every $\frac{1}{3}$ s (i.e., in every tenth video frame). Thus a total of 360 position points were collected for each 2-min test. From every successive pair of position points $[x, y]_i$ and $[x, y]_{i+1}$ the tracking program derived the distance traveled and the bearing between the two points. Angular velocity was calculated as the change in bearing between two successive pairs of points (i.e., the angle defined by $[x, y]_i$, $[x, y]_{i+1}$, and $[x, y]_{i+2}$) divided by the elapsed time. The average number of circles was calculated from the cumulative angle traversed by the mice while swimming.

Experiment 2: c-Fos Induction by Magnetic Field Exposure

Additional mice ($n = 24$) were individually placed in a restraint tube and then exposed to the 14.1-T magnetic field while oriented in one of three positions: head-up toward B+ with rostral-caudal axis parallel to the magnetic field lines (0°); sideways with their dorsal side toward B+ and their ventral side toward B− (90°, perpendicular to the magnet field lines); or head-down with their head toward B− (180°). Six mice were exposed at each orientation. After 15 min of exposure to 14.1 T, the mice were removed from the magnet and returned to their home cages.

As sham controls, additional mice were restrained and placed head-up ($n = 3$) or head-down ($n = 3$) in the sham-magnet for 15 min, then returned to their home cage.

One hour after magnet or sham exposure, mice were overdosed with sodium pentobarbital. When completely unresponsive, the mice were perfused transcardially, first with 100 ml of isotonic saline-0.5% sodium nitrite-1,000 U heparin, and then with 400 ml phosphate-buffered 4% paraformaldehyde. The brains were removed, blocked, postfixed for 24 h, and then transferred into 30% sucrose at 4°C for 24 h to 1 wk before sectioning. Tissue from all treatment groups was processed in parallel.

Coronal sections (40 μm) were cut on a freezing, sliding microtome. The right side of each brain stem was marked by a needle puncture. Alternate sections were processed from the medulla at the level of the nucleus of solitary tract (NTS; bregma −7.64 mm) through the prepositus and medial vestibular nuclei (to bregma −6.24 mm), and through the pons at the level of the supragenualis (bregma −5.8 to −5.68 mm) and parabrachial nucleus (PBN; bregma −5.34 to −5.20 mm). Coordinates were based on those in the atlas by Paxinos and Franklin (23). Sections were immediately processed after cutting for c-Fos immunohistochemistry.

Free-floating tissue sections were washed twice for 15 min in 0.1 M phosphate-buffered saline (PBS) and then incubated for 30 min in 0.2% Triton X-100–1% BSA-PBS. After two washes in PBS/BSA for 15 min each, sections were incubated overnight with a rabbit anti-c-Fos antiserum (Ab-5; Oncogene Research) at a dilution of 1:20,000. After two 15-min washes in PBS/BSA, sections were then incubated for 1 h with a biotinylated goat anti-rabbit antibody (Vector Laboratories) at a dilution of 1:200. Antibody complexes were amplified using the Elite Vectastain ABC kit (Vector Laboratories), and visualized via a 5-min reaction in 0.05% 3,3-diaminobenzidine tetrahydrochloride. Sections were stored in 0.1 M PBS until mounted onto gelatin-coated glass slides, counterstained with methyl green (Vector Laboratories), and coverslipped using Permount.

Cells expressing darkly positive, nuclear c-Fos immunoreactivity were quantified using a custom software program (MindsEye 1.19b; T. Houpt). Images were digitally captured in a 0.72 × 0.54 mm counting frame. Cell counts were restricted to three brain stem nuclei associated with vestibular responses (prepositus, 10 ± 1 sections; medial vestibular, 14 ± 1 sections; and supragenualis, 3 ± 0 sections) and three nuclei associated with visceral and stress responses (medial NTS, 7 ± 1 sections; locus ceruleus, 3 ± 0 sections; and lateral PBN, 5 ± 0 sections). These six regions were delineated by a hand-drawn outline on the left and right sides of the brain stem. The individual mean counts per section for each region were averaged within each mouse and then averaged across mice within experimental groups.

Asymmetry of c-Fos counts for each brain region are presented by subtracting the c-Fos count for the left side of each brain section from the c-Fos count on the right side. Paired *t*-tests were used to compare average c-Fos counts on the left versus right sides of each brain region across the mice within each group (i.e., for each mouse, the average c-Fos count for the left side of a brain region was paired with the count for its own right side).

Statistical Analysis

Data are presented as means ± SE. *t*-Tests, one-way ANOVAs, and Tukey's post hoc comparisons were performed using Kaleidagraph software (Synergy Software).

RESULTS

Experiment 1: Swimming After Magnet Exposure

Fifteen minutes of exposure to 14.1 T induced a significant level of circular swimming in mice oriented at 0° and 180°, but not at 45°, 90°, or 135° (see example tracings of mice swimming in Fig. 2). No significant differences were found between the head-up and head-down sham-exposed groups ($n = 3$ each), so their data were combined into a single sham-exposed group ($n = 6$).

One-way ANOVA across the five groups (sham, 0°, 45°, 90°, 135°, and 180°) showed a significant effect of exposure on total distance swum ($F(5,30) = 8.90$, $P < 0.0001$; Fig. 3*A*), Average angular velocity while swimming ($F(5,30) = 14.0$; $P < 0.0001$; Fig. 3*B*), and cumulative number of circles ($F(5,30) = 14.0$; $P < 0.0001$; Fig. 3*C*). Sham-exposed mice swam in straight lines or broad curves until reaching the side of the swimming pool. Mice exposed at 0°, 45°, and 180° showed a reduced distance of swimming. Mice exposed at 0° and 45° swam on average counterclockwise, whereas mice exposed at 135° and 180° swam clockwise. In particular, mice exposed at 0° and 180° swam in bursts of tight circles, interposed with brief bouts of straight swimming. Although the 0° and 180° groups circled in opposite directions, there was no significant

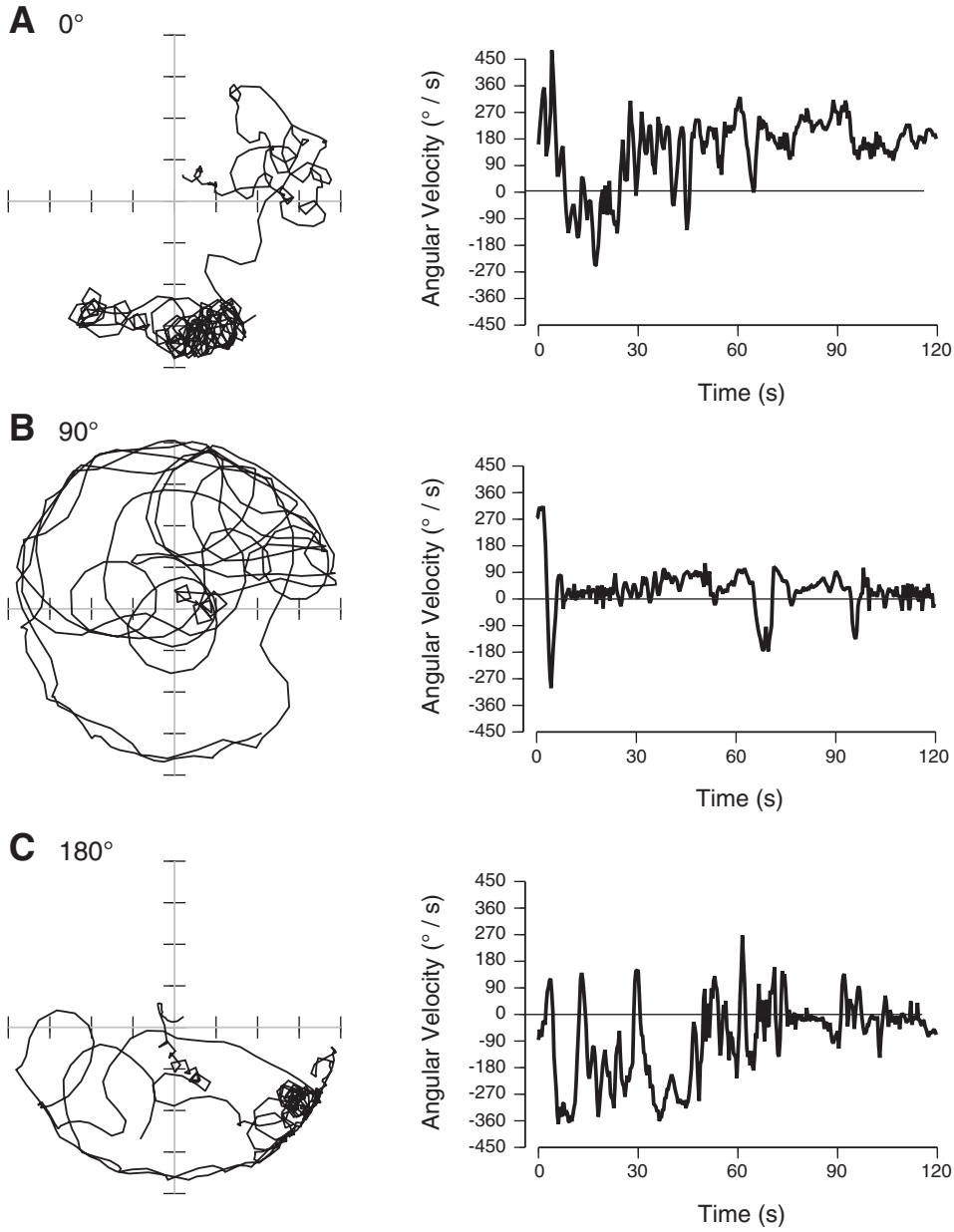

Fig. 2. Example traces of mice swimming after exposure to the magnetic field while oriented at 0° (*A*), 90° (*B*), and 180° (*C*) relative to the magnetic field. *Left:* computer-generated tracks of mice during 2-min swimming test. *Right:* angular velocity of the same mice during the test. Note that mice exposed at 0° and 180° show tight circling with very few linear excursions within the pool; however, the mice swam in opposite directions, with positive (counterclockwise) angular velocity in *A* and negative (clockwise) angular velocity in *C*. The mouse exposed at 90° (*B*) showed long periods of swimming with an average angular velocity close to 0°/s.

difference between those groups in the absolute number of circles when assessed by *t*-test.

Mice exposed at 90° did not swim differently from sham-exposed mice. Similarly, mice exposed on their side at 90° (90° sideways group) swam close to the same distance (20.8 ± 1.8 m) and the same number of circles (2.5 ± 4.1) as sham-exposed mice.

Experiment 2: c-Fos Induction

Examples of c-Fos induction can be seen in Fig. 4 for the prepositus and medial vestibular nuclei, in Fig. 5 for the supragenualis nucleus, and Fig. 6 for the NTS.

Vestibular nuclei. One-way ANOVA of bilateral c-Fos induction across the four groups (sham-exposed; and magnet-exposed at 0°, 90°, and 180°) revealed a significant effect of group for all three vestibular nuclei: prepositus, $F(3,20) = 38.74$, $P < 0.0001$; medial vestibular, $F(3,20) = 15.37$, $P < 0.0001$; and supragenualis, $F(3,20) = 49.56$, $P < 0.0001$ (see Fig. 7, *top*). Mice exposed in the magnet at 0° and 180° showed significantly more c-Fos expression in vestibular regions than sham-exposed mice. However, c-Fos counts in mice exposed in the magnet at 90° were not different from those in sham-exposed mice.

Mice exposed to the magnet field at 0° and 180° also showed significant asymmetry in c-Fos expression in the three vestibular nuclei, but in opposite directions (See Fig. 7, *bottom*). By paired *t*-test, mice exposed at 0° had more c-Fos on the left side of the brain stem in the medial vestibular and supragenualis, whereas mice exposed at 180° had more c-Fos on the right side of the brain stem in all three nuclei. Both sham-exposed mice and mice exposed at 90° did not show significant asymmetry in c-Fos expression.

Visceral nuclei. One-way ANOVA of bilateral c-Fos induction across the four groups (sham-exposed; and magnet-ex-

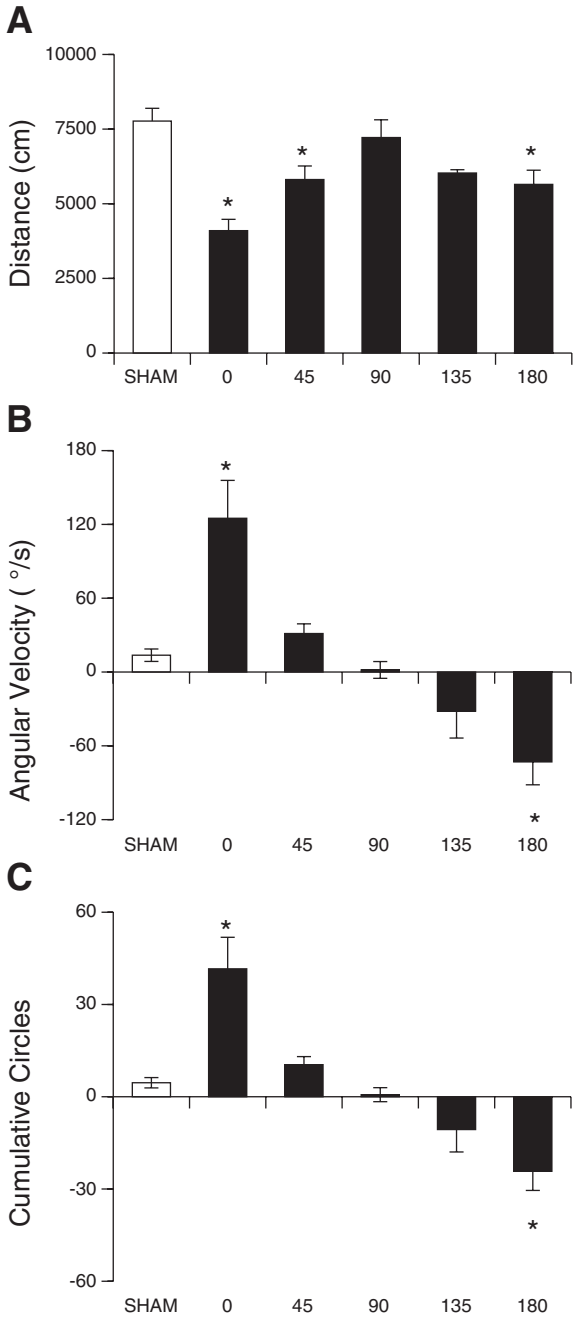

Fig. 3. Mean distance (*A*), angular velocity (*B*), and cumulative circles (*C*) during 2-min swimming test of mice after sham exposure or 15-min exposure to 14.1 T while oriented at different angles relative to the magnetic field. Maximal suppression of distance traveled, maximal turning rate, and maximal circling were observed in mice exposed at 0° and 180° (parallel to the magnetic field). However, mice at 0° and 180° circled in opposite directions. Mice exposed at 90° (perpendicular to the magnetic field) did not swim differently than sham-exposed mice. *$P < 0.05$ vs. sham-exposed mice.

posed at 0°, 90°, and 180°) revealed a significant effect of group for all three visceral nuclei: NTS, $F(3,20) = 21.86$, $P < 0.0001$; locus ceruleus, $F(3,20) = 4.29$, $P < 0.01$, $P < 0.0001$; lateral PBN, $F(3,20) = 7.57$, $P < 0.005$ (see Fig. 8, *top*). In the vestibular nuclei, visceral regions of mice exposed to the magnetic field at 0° or 180° tended to show significantly more c-Fos than sham-exposed mice. Levels of c-Fos in the NTS, locus ceruleus, and PBN of mice exposed at 90° were not significantly different from those in sham-exposed mice.

Paired *t*-tests comparing left-side vs. right-side expression of c-Fos found significant asymmetry of c-Fos counts in all three visceral regions (see Fig. 8, *bottom*). Unlike the vestibular regions, however, the pattern of left versus right c-Fos induction did not appear related to orientation during magnet exposure. Mice tended to have more c-Fos on the left side of the NTS, but on the right side of the locus ceruleus and lateral PBN, regardless of treatment.

DISCUSSION

Summary

In this study we tested the effect of varying the angle of orientation of mice during their exposure to a static, high magnetic field, measuring response as angular velocity and circling during a postexposure swim test and by measuring c-Fos induction in the brain stem 1 h after exposure. Assuming that the intensity of circling (i.e., average angular velocity and total number of circles during the 2-min swimming test) and number of c-Fos-positive cells reflects the strength of vestibular stimulation during exposure to the high magnetic field, then maximal stimulation was achieved when the rostral-caudal axis was parallel to the magnetic field (at 0° and 180°). The lack of significant circling and c-Fos induction after exposure at 90° defined a null point for magnetic field stimulation. These results extend our earlier observation that rats exposed perpendicular to the field of a large, resistive magnet did not circle and did not acquire significant CTA (17). Because the conical restraint tubes made the plane of the horizontal canal and utricle parallel to the field at 0° and perpendicular at 90°, these results suggest that the magnetic field interacts with these components of the peripheral vestibular apparatus.

Circular swimming. We have consistently observed that rats and mice circle counterclockwise after exposure with their head toward B+, but circle clockwise when exposed with their head toward B−. This relation holds both when the animal is inverted (head-down) relative to the field, and when the magnetic field is inverted with the animal held head-up. The circling is observed when animals walk in a test chamber but is more pronounced when activity is elicited by swimming. The circling and other postural deficits persist for less than 10 min after removal from the magnet (15). In this study, the induction of circular swimming varied with the angle of exposure, with a graded response from maximum at 0° to a minimum at 90°, back to maximal response at 180°. The direction of circling also reversed from counterclockwise when oriented head-up to clockwise when head-down, with the reversal point apparently at 90°.

The locomotor circling is likely the result of reflexive responses to vestibular stimulation by the magnetic field. We have observed that during head-up (0°) exposure to the magnetic field rats tilt their head to the right, which induces circling immediately after exposure to the left (13). The responses were reversed when rats were exposed head-down (at 180°). Interestingly, magnet field exposure induces nystagmus in humans (21, 24), and the direction of nystagmus can be reversed by reversing head orientation within the magnet (24). We interpret the head tilt during magnetic field exposure as a vestibulocollic

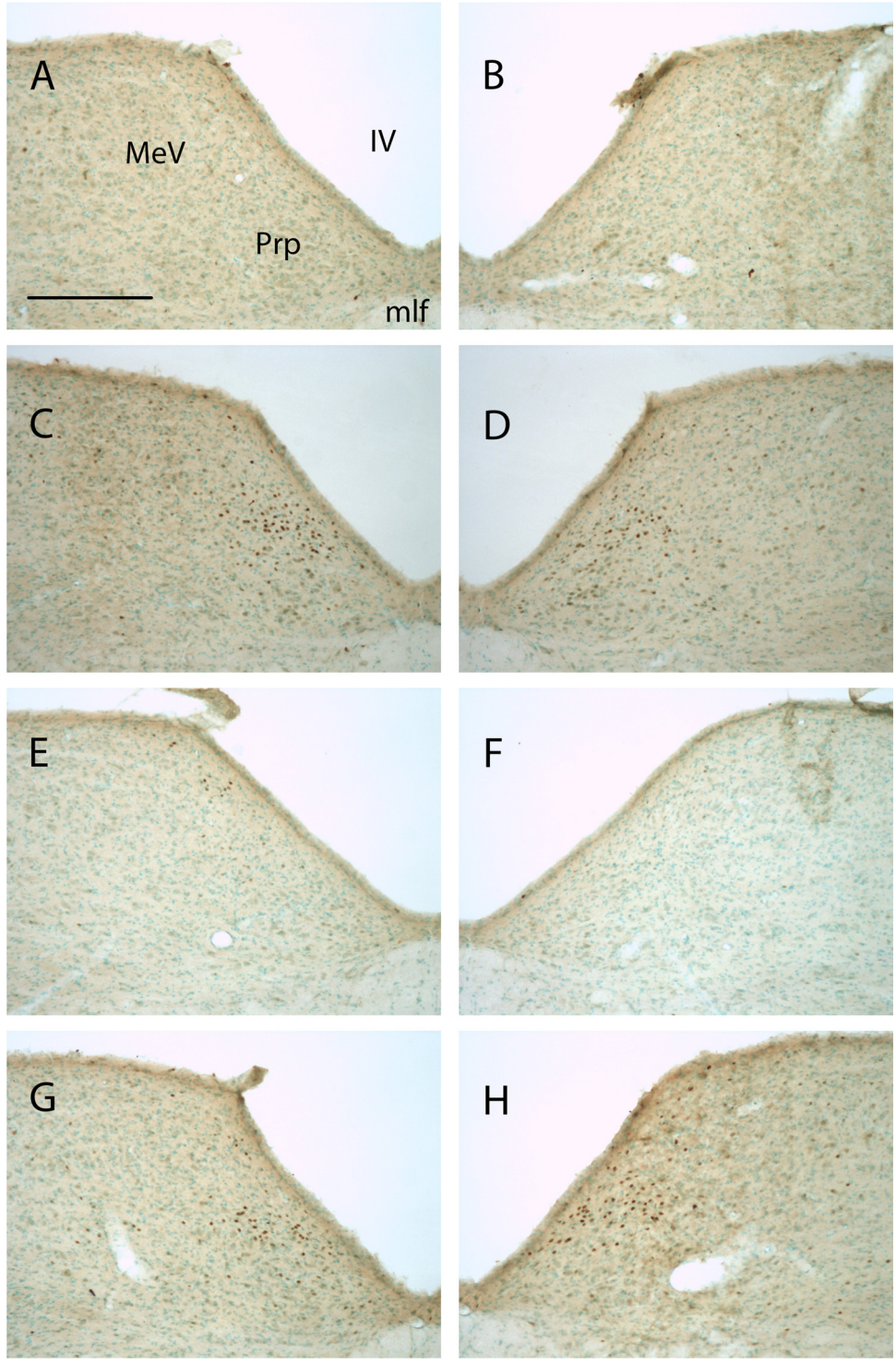

Fig. 4. Photomicrographs of c-Fos immunohistochemistry in coronal sections through the left (*A, C, E, G*) and right (*B, D, F, H*) dorsal medulla of a sham-exposed mouse (*A, B*), and in mice 1 h after exposure to 14.1 T while oriented at 0° (*C, D*), 90° (*E, F*), and 180° (*G, H*) relative to the magnetic field. Significant c-Fos was induced in the prepositus (Prp) nuclei and medial vestibular nuclei (MeV) after magnetic field exposure at 0° and 180° but not at 90°. Furthermore, significantly more c-Fos was induced on the left side of the MeV after exposure at 0°, and significantly more c-Fos was induced on the right side of the Prp and MeV after exposure at 180°. IV, fourth ventricle; mlf, medial longitudinal fasciculus. Scale bar, 200 μm.

reflex to a magnetically evoked vestibular stimulus: if the rat perceives an illusory fall leftward, for example, then it would reflexively tilt its head in the opposite direction to the right.

We then interpret the locomotor circling immediately after exposure as a compensatory response to the removal of the persistent vestibular perturbation imposed during magnetic field exposure: having tilted to the right during exposure, the rat turns to the left when relieved of stimulation. Similarly, the direction of nystagmus induced during magnetic field exposure reverses when human subjects are removed from the bore of the magnet (24). Presumably the same reflexes are invoked in mice during and after restraint in conical tubes within the magnetic field. The possible mechanism for inducing leftward versus rightward stimulation at the level of the horizontal canal depending on orientation is discussed below.

c-Fos induction. The neural response of the brain stem to magnetic field exposure paralleled the behavioral response of mice in both magnitude and orientation. In the vestibular nuclei

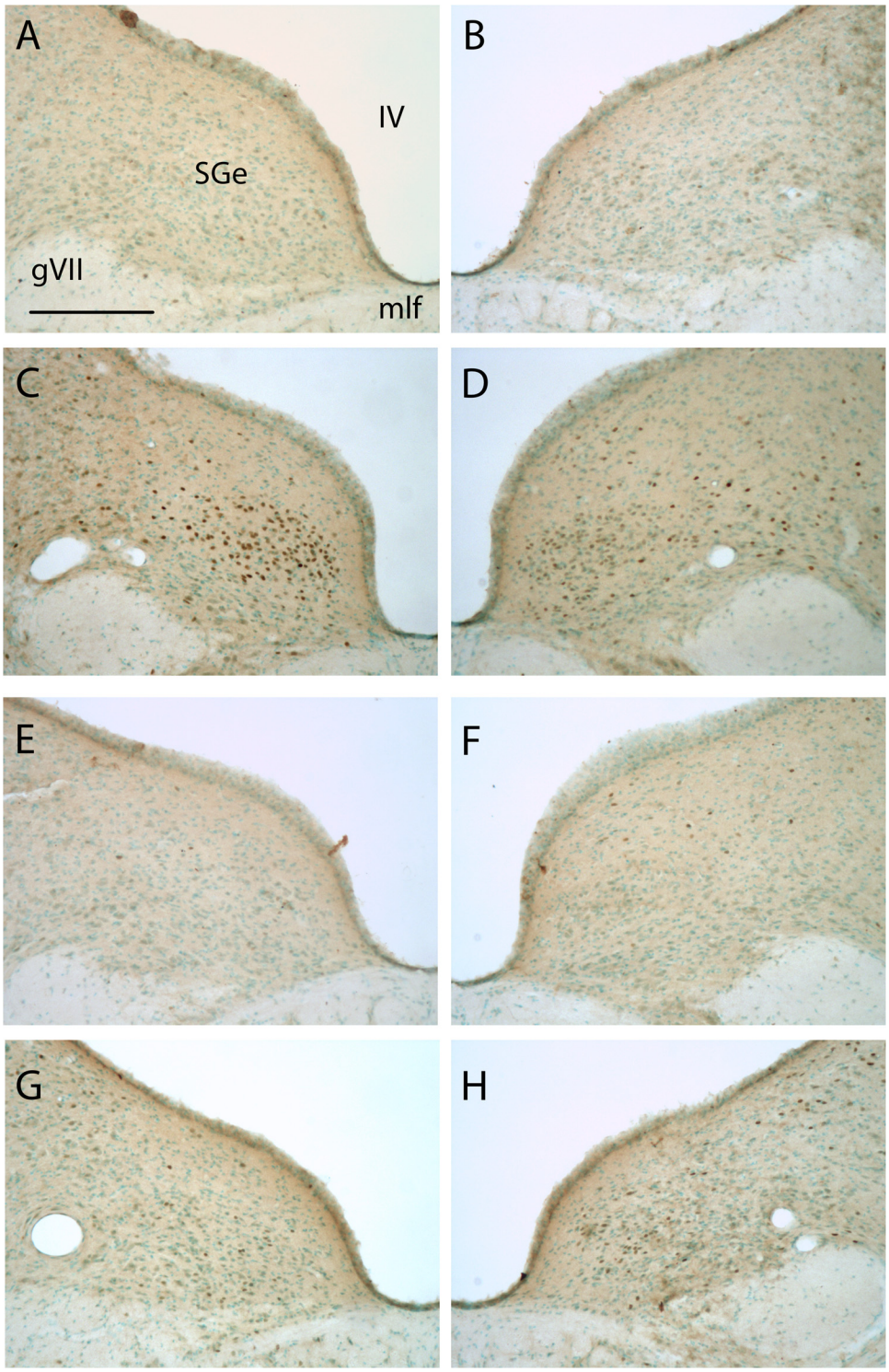

Fig. 5. Photomicrographs of c-Fos immunohistochemistry in coronal sections through the left (*A, C, E, G*) and right (*B, D, F, H*) dorsomedial pons of a sham-exposed mouse (*A, B*), and in mice 1 h after exposure to 14.1 T while oriented at 0° (*C, D*), 90° (*E, F*), and 180° (*G, H*) relative to the magnetic field. Significant c-Fos was induced in the supragenualis nuclei (SGe) after magnetic field exposure at 0° and 180° but not at 90°. Furthermore, significantly more c-Fos was induced on the left side of the SGe after exposure at 0°, and significantly more c-Fos was induced on the right side after exposure at 180°. IV, fourth ventricle; gVII, genu of the facial nerve; mlf, medial longitudinal fasciculus. Scale bar, 200 μm.

and two of the three visceral nuclei, magnetic field exposure induced significantly greater c-Fos-positive cells than sham exposure when mice were exposed parallel to the magnetic field (at 0° and 180°), but not when exposed perpendicular to the field (at 90°). Furthermore, exposure at 0° induced more c-Fos in the left vestibular nuclei, whereas exposure at 180° induced significantly more c-Fos in the right vestibular nuclei. Previously, we have reported some asymmetrical c-Fos induction after 30-min head-up exposure to 14.1 T in ovariectomized female rats (with modulation by estrogen replacement), although the lateralization was not as robust as observed here in mice (3).

Also consistent with earlier findings (3, 28), magnetic field exposure induced c-Fos in visceral relays of the brain stem. The induction by magnetic field exposure at 0° and 180° was significantly greater than the c-Fos induced by restraint stress

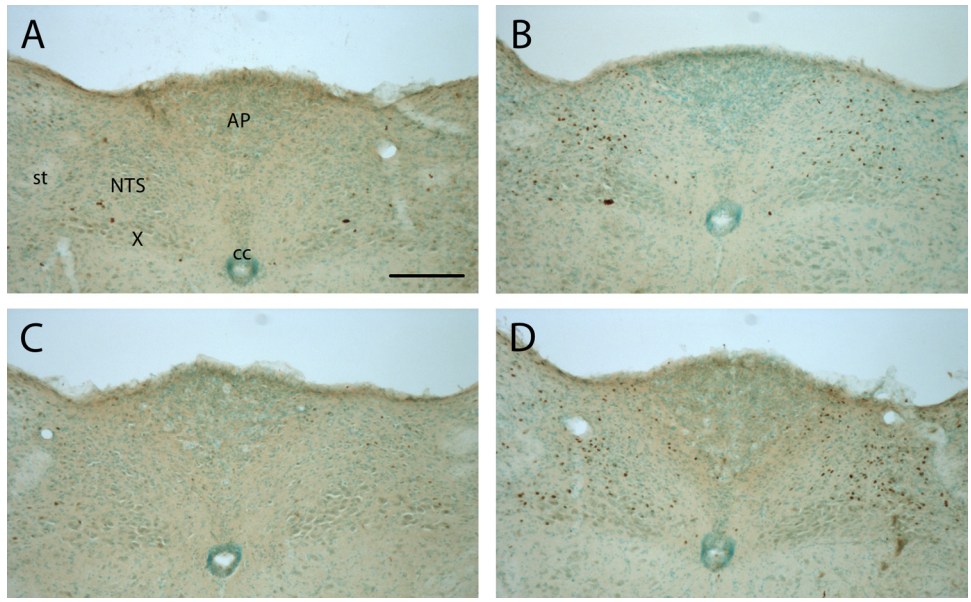

Fig. 6. Photomicrographs of c-Fos immunohistochemistry in coronal sections through dorsal medulla of a sham-exposed mouse (*A*), and in mice 1 h after exposure to 14.1 T while oriented at 0° (*B*), 90° (*C*), and 180° (*D*) relative to the magnetic field. Significant c-Fos was induced in the NTS after magnetic field exposure at 0° and 180° but not at 90°. No left-right differences were found. NTS, nucleus of the solitary tract; AP, area postrema; st, solitary tract; cc, central canal. Scale bar, 200 μm.

alone in the sham controls. Activation of visceral nuclei might reflect additional stress of magnetic field exposure. However, the dependence of c-Fos induction in the NTS and lateral PBN on the angle of exposure suggests a vestibular contribution to visceral activation (25). Although some laterality of c-Fos expression was found in the visceral nuclei, it did not vary with orientation during exposure.

It is notable that c-Fos induced in the left vestibular nuclei induced by magnetic field exposure paralleled the induction, after removal from the magnet, of swimming counterclockwise to the left, whereas c-Fos induction on the right side paralleled postexposure swimming clockwise to the right. (Because separate mice were assessed for c-Fos induction and swimming, we can conclude that the c-Fos is induced by magnet exposure and not by the postexposure swimming.) Combined with our report that rats tilt their head during exposure in the opposite direction of their postexposure circling (13), this suggests that asymmetrical activation of the vestibular system during mag-

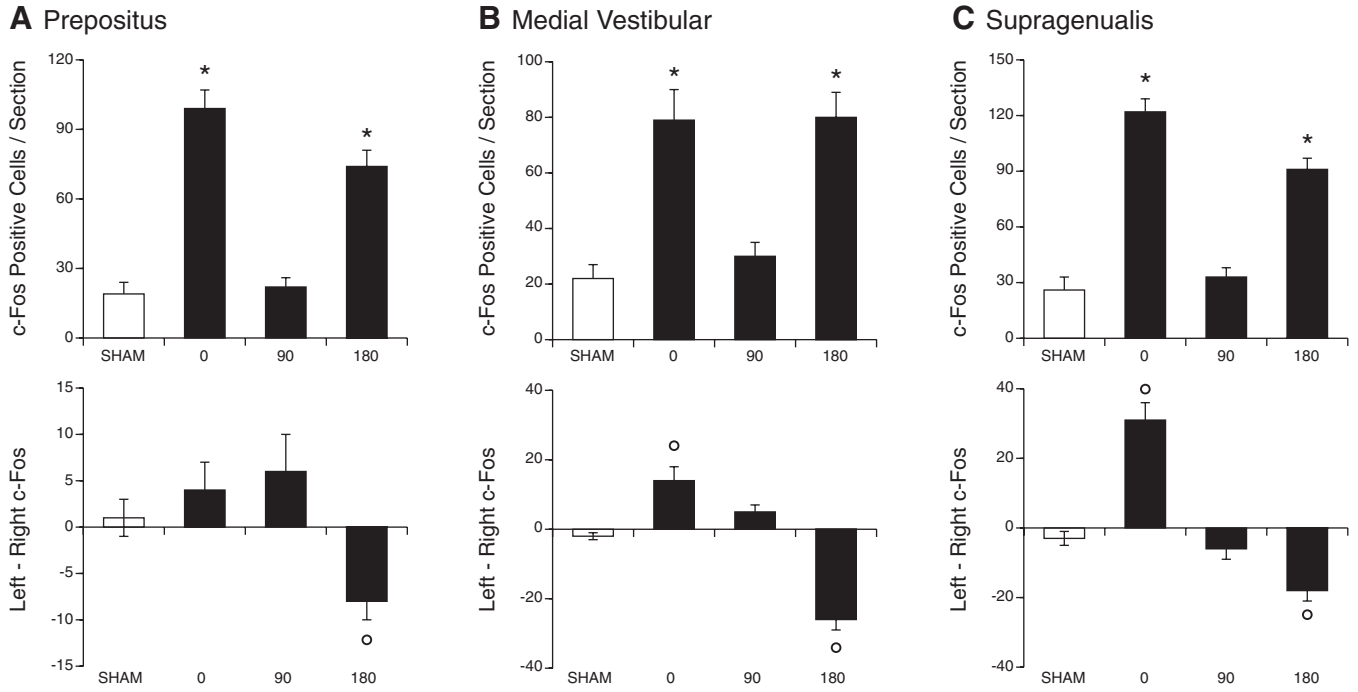

Fig. 7. Quantification of c-Fos-positive cells in vestibular nuclei of the brain stem after sham exposure or 15-min exposure to 14.1 T while oriented at 0°, 90°, or 180° relative to the magnetic field lines. *Top*: bilateral counts of c-Fos-positive cells; *bottom*: laterality of c-Fos counts expressed as (left-side counts) − (right-side counts). Magnet exposure induced significant c-Fos in the prepositus (*A*), medial vestibular (*B*), and supragenualis (*C*) nuclei of mice oriented at 0° and 180°, but not 90°. Furthermore, significantly more c-Fos was found on the left side of mice exposed at 0° in the medial vestibular and supragenualis nuclei, whereas more c-Fos was found on the right side of all three nuclei in mice exposed at 180°. *$P < 0.05$ vs. sham-exposed mice; ○$P < 0.05$ vs. opposite side by paired *t*-test.

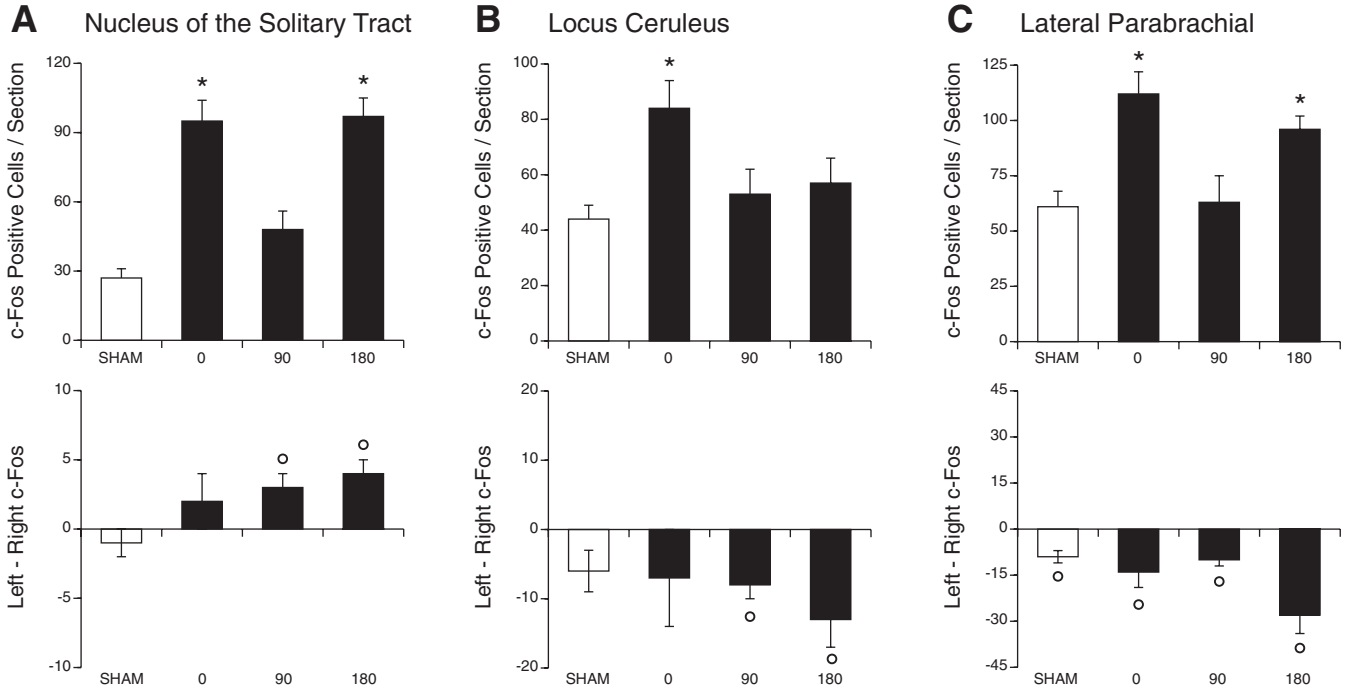

Fig. 8. Quantification of c-Fos-positive cells in visceral nuclei of the brain stem after sham exposure or 15-min exposure to 14.1 T while oriented at 0°, 90°, or 180° relative to the magnetic field lines. *Top*: bilateral counts of c-Fos-positive cells; *bottom*: laterality of c-Fos counts expressed as (left-side counts) − (right-side counts). Magnet exposure induced significant c-Fos in the nucleus of the solitary tract (*A*), locus ceruleus (*B*; 0° only), and lateral parabrachial (*C*) nuclei of mice oriented at 0° and 180°, but not 90°. Although some laterality of c-Fos expression was observed in all three nuclei, the pattern of left vs. right c-Fos expression was similar across all magnet exposures. *$P < 0.05$ vs. sham-exposed mice; ○$P < 0.05$ vs. opposite side by paired *t*-test.

netic field exposure leads to head movements during exposure, which are turned away from the side of greatest activation, and postexposure locomotor turning toward the side of greatest activation.

The c-Fos results are consistent with the magnetic field applying asymmetric stimulation (or inhibition) to the two inner ears. Asymmetric c-Fos patterns have been reported by others after asymmetric treatments [e.g., unilateral electrical stimulation or hemilabyrinthectomy (19)]. We do not believe that the c-Fos is induced by the circular locomotion per se observed after magnetic field exposure; we have unpublished data showing that the same pattern of c-Fos is observed if rats are kept restrained after exposure until the circling behavior wears off. It is a logical possibility that the vestibular system is more activated by the release from stimulation when removed from the magnet than it is by the exposure itself (or indeed the vestibular system might be more activated by the transition from the high magnetic field back to ambient conditions). However, the behavioral effects are largely correlated with duration of exposure, not with movement in and out of the magnet (12, 16). However, the release from stimulation upon removal from the magnet would seem to be concomitant with any discrete period of stimulation within the magnet, and so may not be separable.

Angle variation. Vestibular responses to high magnetic field exposure depends on an intact peripheral vestibular system in both rats (2) and humans (24). We probed the contributing components of the vestibular systems by varying the angle at which the mice were positioned in the magnet, and thus orienting the components of the vestibular apparatus (semicircular canals, saccule, and utricle) at different angles relative to the magnetic field.

In particular, the null point with the mouse positioned at 90° relative to the magnetic field placed the plane of the horizontal canal and utricle perpendicular to the field. As in rats, guinea pigs, and humans, the horizontal canal and utricle in the C57 mouse is pitched up rostrally from the horizontal plane by ~30° (1). When our mice were restrained in a conical tube, the head of the mouse was pitched down rostrally by 30°, bringing the horizontal canal and utricle parallel to the horizontal plane. Thus at 0° and 180° positions (the maximally effective positions) compared with the 90° position (the null point), the horizontal canal and utricle were parallel vs. perpendicular to the magnetic field, respectively. This is suggestive, insofar as the magnetic field might be expected to induce a force or torque at right angles to the field lines (i.e., at 0° and 180° the force would be directed in the plane of the horizontal canal and utricle).

Model mechanisms. Several models have been proposed for how the magnetic field might influence the vestibular system, including magnetohydrodynamic force (27), galvanic stimulation (10), or otoconia interactions (10). Our results are consistent with the mechanism proposed by Roberts et al. (24), who suggest that the magnetic field induces a Lorentz force on the endolymph of the horizontal canal due to the interaction of the field with the K^+ current across the duct. Briefly, a dorsoventral flow of K^+ ions into the horizontal ampulla and utricular hair cells may act as a current through the conductive endolymph. When positioned perpendicular to the magnetic field lines, then a Lorentz force would be imposed perpendicular to both the magnetic field and the current flow (by the right-hand rule). This force would move the endolymph and deform the cupula, thus stimulating the horizontal canal input to the

vestibular system. Our results are also consistent with a role for the utricle, which lies in the same plane as the horizontal canal.

Importantly, the direction of the force predicted by the Lorentz force model would be reversed if the relative direction of the magnetic field was reversed. Thus the model predicts the direction of nystagmus observed in humans by Roberts et al. and is consistent with the reversal of the direction of the nystagmus when the orientation of the head is reversed, or when the head is pitched anteriorly up (and back) versus pitched anteriorly down (and forward).

Four points summarize the application of this model to our current results with mice, assuming a dorsoventral flow of K^+ (the current) perpendicular to the plane of the horizontal canal and utricle: *1*) at 0°, the dorsoventral current is perpendicular to the (rostrocaudal) magnetic field, so the Lorentz force would be in horizontal plane directed toward the left; *2*) at 90°, the dorsoventral current is parallel to the (ventrodorsal) magnetic field, so no Lorentz force is induced; *3*) at 90° sideways, the dorsoventral current is perpendicular to the (mediolateral) magnetic field, so the Lorentz force would be in the horizontal plane but directed caudally, which would have minimal impact on the horizontal ampulla; and *4*) at 180°, the dorsoventral current is perpendicular to the (caudorostral) magnetic field, so the Lorentz force would be in the horizontal plane toward the right.

Although stated in the context of the model of Roberts et al., these spatial orientations of the vestibular apparatus relative to the magnetic field may be relevant in other models as well.

There appears to be little contribution from the other canals. At 0° and 180° orientations, the horizontal canals are parallel to the magnetic field. At orientations other than 0° and 180°, however, one of the vertical canal pairs should be positioned parallel to the field, yet only submaximal responses were observed in swimming and c-Fos induction when the vertical canals were parallel to the magnetic field. A Lorentz force should also be acting on the vertical canals in these positions. However, the response may be of lower magnitude or absent compared with horizontal canal stimulation.

It will be difficult to verify a specific mechanism for the interaction of a high magnetic field with the vestibular apparatus. For example, the Lorentz force model depends on a coherent current carried by K^+ ions flowing predominately in the dorsoventral direction across the height of the horizontal duct. However, K^+ secretion into the vestibular endolymph arises from dark cells adjacent to the hair cells on the ventral surface of the horizontal duct (11). Because activation of the vestibular hair cells depends on K^+ influx, attempting to remove the Lorentz force by abolishing the K^+ current would be confounded by the simultaneous loss of sensory transduction by the hair cells.

Perspectives and Significance

Static high-magnetic fields >7 T, as employed in MRI studies, can perturb the vestibular apparatus of the inner ear in humans and rodents. The effect is dependent on the orientation of the inner ear with respect to the magnetic field. The present results point to the horizontal elements of the inner ear (the horizontal canal or the utricle) as the locus of magnetic field effects. Several models have been proposed for how a magnetic field might cause vestibular stimulation, in particular the model of Roberts et al., which proposes that the magnetic field induces a Lorenz force that deflects the horizontal cupola. Future studies will need to test models by localizing magnetic field effects to specific inner ear elements by ablation, because limited, site-specific application of a high-magnetic field is not possible.

ACKNOWLEDGMENTS

We thank Drs. Timothy Cross and Zhehong Gan of the United States National Magnetic Field Laboratory for providing access to the magnet, and Dr. Michael Meredith for helpful discussions.

GRANTS

Supported by National Institute on Deafness and Other Communication Disorders Grant R01 DC-4607.

DISCLOSURES

No conflicts of interest, financial or otherwise, are declared by the author(s).

AUTHOR CONTRIBUTIONS

Author contributions: T.A.H., B.K., C.E.H., and J.C.S. conception and design of research; T.A.H., B.K., C.E.H., B.N., and J.C.S. performed experiments; T.A.H., B.K., C.E.H., and J.C.S. analyzed data; T.A.H., B.K., C.E.H., and J.C.S. interpreted results of experiments; T.A.H. and C.E.H. prepared figures; T.A.H. drafted manuscript; T.A.H. and J.C.S. edited and revised manuscript; T.A.H. and J.C.S. approved final version of manuscript.

REFERENCES

1. **Calabrese DR, Hullar TE.** Planar relationships of the semicircular canals in two strains of mice. *J Assoc Res Otolaryngol* 7: 151–159, 2006.
2. **Cason AM, Kwon B, Smith JC, Houpt TA.** Labyrinthectomy abolishes the behavioral and neural response of rats to a high-strength static magnetic field. *Physiol Behav* 97: 36–43, 2009.
3. **Cason AM, Kwon B, Smith JC, Houpt TA.** c-Fos induction by a 14 T magnetic field in visceral and vestibular relays of the female rat brainstem is modulated by estradiol. *Brain Res* 1347: 48–57, 2010.
4. **Chakeres DW, Bornstein R, Kangarlu A.** Randomized comparison of cognitive function in humans at 0 and 8 Tesla. *J Magn Reson Imaging* 18: 342–345, 2003.
5. **Chakeres DW, Kangarlu A, Boudoulas H, Young DC.** Effect of static magnetic field exposure of up to 8 Tesla on sequential human vital sign measurements. *J Magn Reson Imaging* 18: 346–352, 2003.
6. **de Vocht F, Glover P, Engels H, Kromhout H.** Pooled analyses of effects on visual and visuomotor performance from exposure to magnetic stray fields from MRI scanners: application of the Bayesian framework. *J Magn Reson Imaging* 26: 1255–1260, 2007.
7. **de Vocht F, Stevens T, van Wendel-de-Joode B., Engels H., Kromhout H.** Acute neurobehavioral effects of exposure to static magnetic fields: analyses of exposure-response relations. *J Magn Reson Imaging* 23: 291–297, 2006.
8. **de Vocht F, van Drooge H, Engels H, Kromhout H.** Exposure, health complaints and cognitive performance among employees of an MRI scanners manufacturing department. *J Magn Reson Imaging* 23: 197–204, 2006.
9. **de Vocht F, van-Wendel-de-Joode B, Engels H, Kromhout H.** Neurobehavioral effects among subjects exposed to high static and gradient magnetic fields from a 15 Tesla magnetic resonance imaging system–a case-crossover pilot study. *Magn Reson Med* 50: 670–674, 2003.
10. **Glover PM, Cavin I, Qian W, Bowtell R, Gowland PA.** Magnetic-field-induced vertigo: a theoretical and experimental investigation. *Bioelectromagnetics* 28: 349–361, 2007.
11. **Hibino H, Nin F, Tsuzuki C, Kurachi Y.** How is the highly positive endocochlear potential formed? The specific architecture of the stria vascularis and the roles of the ion-transport apparatus. *Pflugers Arch* 459: 521–533, 2010.
12. **Houpt TA, Carella L, Gonzalez D, Janowitz I, Mueller A, Mueller K, Neth B, Smith JC.** Behavioral effects on rats of motion within a high static magnetic field. *Physiol Behav* 102: 338–346, 2011.

13. **Houpt TA, Cassell J, Carella L, Neth B, Smith JC.** Head tilt in rats during exposure to a high magnetic field. *Physiol Behav* 105: 388–393, 2012.
14. **Houpt TA, Cassell JA, Riccardi C, DenBleyker MD, Hood A, Smith JC.** Rats avoid high magnetic fields: dependence on an intact vestibular system. *Physiol Behav* 92: 741–747, 2007.
15. **Houpt TA, Houpt CE.** Circular swimming in mice after exposure to a high magnetic field. *Physiol Behav* 100: 284–290, 2010.
16. **Houpt TA, Pittman DW, Barranco JM, Brooks EH, Smith JC.** Behavioral effects of high-strength static magnetic fields on rats. *J Neurosci* 23: 1498–1505, 2003.
17. **Houpt TA, Pittman DW, Riccardi C, Cassell JA, Lockwood DR, Barranco JM, Kwon B, Smith JC.** Behavioral effects on rats of high strength magnetic fields generated by a resistive electromagnet. *Physiol Behav* 86: 379–389, 2005.
18. **Kangarlu A, Burgess RE, Zhu H, Nakayama T, Hamlin RL, Abduljalil AM, Robitaille PM.** Cognitive, cardiac, and physiological safety studies in ultra high field magnetic resonance imaging. *Magn Reson Imaging* 17: 1407–1416, 1999.
19. **Kaufman GD, Perachio AA.** Translabyrinth electrical stimulation for the induction of immediate-early genes in the gerbil brainstem. *Brain Res* 646: 345–350, 1994.
20. **Lockwood DR, Kwon B, Smith JC, Houpt TA.** Behavioral effects of static high magnetic fields on unrestrained and restrained mice. *Physiol Behav* 78: 635–640, 2003.
21. **Marcelli V, Esposito F, Aragri A, Furia T, Riccardi P, Tosetti M, Biagi L, Marciano E, Di Salle F.** Spatio-temporal pattern of vestibular information processing after brief caloric stimulation. *Eur J Radiol* 70: 312–316, 2009.
22. **Patel M, Williamsom RA, Dorevitch S, Buchanan S.** Pilot study investigating the effect of the static magnetic field from a 9.4-T MRI on the vestibular system. *J Occup Environ Med* 50: 576–583, 2008.
23. **Paxinos G, Franklin KB.** *The Mouse Brain in Stereotaxic Coordinates*-(Deluxe Edition) (2nd Ed). San Diego, CA: Academic, 2001.
24. **Roberts DC, Marcelli V, Gillen JS, Carey JP, Santina Della CC, Zee DS.** MRI magnetic field stimulates rotational sensors of the brain. *Curr Biol* 21: 1635–1640, 2011.
25. **Ruggiero DA, Mtui EP, Otake K, Anwar M.** Vestibular afferents to the dorsal vagal complex: substrate for vestibular-autonomic interactions in the rat. *Brain Res* 743: 294–302, 1996.
26. **Schenck JF, Dumoulin CL, Redington RW, Kressel HY, Elliott RT, McDougall IL.** Human exposure to 4.0-Tesla magnetic fields in a whole-body scanner. *Med Phys* 19: 1089–1098, 1992.
27. **Schenck JF.** Health and physiological effects of human exposure to whole-body four-tesla magnetic fields during MRI. *Ann NY Acad Sci* 649: 285–301, 1992.
28. **Snyder DJ, Jahng JW, Smith JC, Houpt TA.** c-Fos induction in visceral and vestibular nuclei of the rat brain stem by a 9.4 T magnetic field. *Neuroreport* 11: 2681–2685, 2000.
29. **Theysohn JM, Maderwald S, Kraff O, Moenninghoff C, Ladd ME, Ladd SC.** Subjective acceptance of 7 Tesla MRI for human imaging. *MAGMA* 21: 63–72, 2008.
30. **Yang M, Christoforidis G, Abduljali A, Beversdorf D.** Vital signs investigation in subjects undergoing MR imaging at 8T. *Am J Neuroradiol* 27: 922–928, 2006.